IEEE Access
Multidisciplinary | Rapid Review | Open Access Journal

Received February 20, 2021, accepted March 14, 2021, date of publication March 22, 2021, date of current version March 29, 2021.

Digital Object Identifier 10.1109/ACCESS.2021.3067720

A Piezoelectric Linear Actuator Controlled by the Reversed-Phase Connection of Two Bimorphs

TIANYU JIANG, JIJIE MA, YILI HU, QITAO LU, JIANPING LI, AND JIANMING WEN

Key Laboratory of Urban Rail Transit Intelligent Operation and Maintenance Technology and Equipment of Zhejiang Province, Zhejiang Normal University, Zhejiang 321005, China

College of Engineering, Institute of Precision Machinery and Smart Structure, Zhejiang Normal University, Jinhua 321004, China

Corresponding authors: Jijie Ma (mjj@zjnu.cn) and Jianming Wen (wjming@zjnu.cn)

This work was supported in part by the Natural Science Foundation of Zhejiang Province under Project LY20E050009 and Project LQ21E050013, and in part by the Zhejiang Provincial Key Research and Development Project of China under Project 2021C01181.

ABSTRACT A linear actuator controlled by the reversed-phase connection of two piezoelectric bimorphs is proposed in this study to solve the problem of drawback in the existing piezoelectric linear actuators. The actuator is driven by one excitation signal, the two piezoelectric bimorphs will always bend in opposite directions by the reversed-phase connection, so the directions of the force output by the two piezoelectric bimorphs are opposite. Because of the length difference of the clamping blocks, the two forces outputted by each bending is different in magnitude, and always have a resultant force in the same direction to make the actuator move forward two steps in one cycle without drawback. A series of experiments were conducted to evaluate the performance of the actuator provided. The starting voltage is 40 V_{p-p}, resolution can reach 1.16μm without load. The load capacity of the actuator is 450 g with a 100 V_{p-p} voltage, a 2-Hz frequency, and the average step displacement in this case is 0.725 μm. The prototype has high linearity and good repeatability. Experiments have proved that the actuator controlled by reversed-phase connection can eliminate drawback in principle, and can move forward two steps in one cycle. The resolution of the prototype by the reversed-phase connection is much higher than the in-phase connection, and it is a new method to improve the driving performance of piezoelectric actuators.

INDEX TERMS Actuator, drawback, piezoelectric, reversed-phase connection.

I. INTRODUCTION

In recent years, inertial piezoelectric actuators have been widely used in robots [1]–[3], biological engineering [4]–[6], optics [7]–[9], and ultra-precision machining [10]–[12] fields because of their simple structure, large stroke and high precision.

Inertial piezoelectric actuators can be divided into signal-control type (SCT), mechanical-control type (MCT) and friction-control type (FCT) according to the control method. The signal control type is to pass an asymmetric signal to the piezoelectric element to make the vibration speed different in two directions, so that the actuator moves different distances in the two directions [13]–[16]. Li *et al.* proposed a parallelogram bending flexure hinge mechanism, which can output a minimum displacement of 0.04 μm with a saw-tooth wave [13]. SCT has the advantage of high positioning accuracy, but it involves a signal generator to generate the asymmetric signal. Similar to SCT, MCT also moves the actuator with asymmetric driving force. But the travel difference comes from the asymmetric structure [17]–[21]. Shen *et al.* presented an inertial piezoelectric actuator based on asymmetric clamping materials. A minimum step displacement of the actuator under 2 μm can be achieved under a voltage of 15 V [18]. Bao *et al.* presented an inertial piezoelectric actuator equipped with different combinations of asymmetrical clamping structures and bias unit. At that a voltage of 50 Vp-p, a maximum angular velocity of 18.88 mrad/s and a minimum resolution of 2.8 mrad can be obtained [19]. Instead of asymmetric driving force, FCT actively produces asymmetric friction in the forward and backward direction to generate the travel difference [22]–[25], [31]. Wen *et al.* proposed a new inertial piezoelectric actuator based on the control of the friction force between the rotor and the supporting surface through the use of a triangular block. At that a frequency of 10 Hz and a volage of 15 V_{p-p}, the prototype

The associate editor coordinating the review of this manuscript and approving it for publication was Hui Xie.

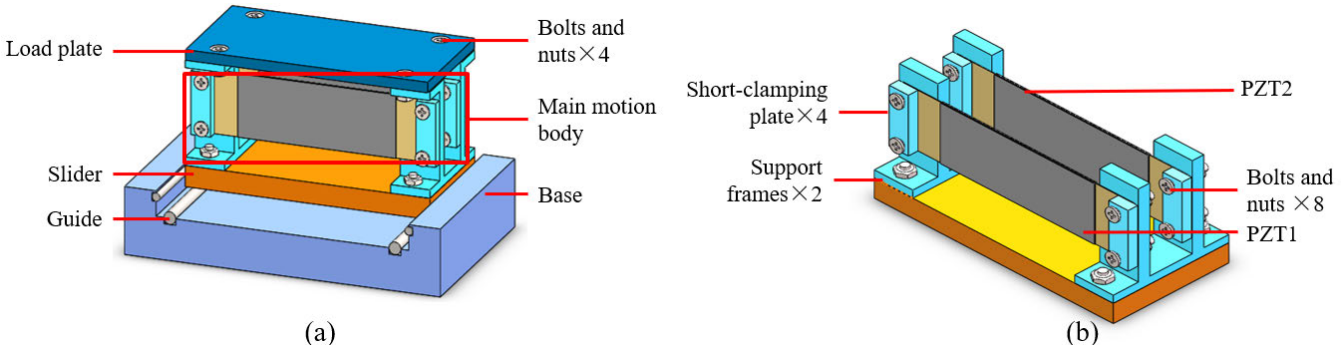

FIGURE 1. (a) Structure of the proposed piezoelectric actuator (b) Main motion body.

reaches the minimum step angle displacement, the minimum step angle displacement is 10 μrad [24].

A common problem of the above inertial piezoelectric actuators is drawback [26]–[28] which reduces the stability of actuators and brings limitations to their applications in critical situations like cell puncture. Theoretically, drawback can be eliminated if friction is greater than the driving force in backward direction. Researchers have originated many ways to eliminate or reduce drawback [29]–[36]. Some researchers adjust the driving force of backward to match to the friction by changing the voltage [22], [24], [29], [30]. Zhang *et al.* adjusted structural parameters and voltage to match friction, which also achieved the goal of no drawback [29]. This method can achieve no backward only when the friction force and the driving force are well adapted, but cannot be universally applied to various actuators. Another way to reduce drawback is to optimize the waveform of the drive signal [25], [31], [32]. Wang *et al.* proposed a driving method realized by a composite waveform which consists of a saw-tooth driving wave and a sinusoidal friction driving wave for backward motion restraint of the actuator [31]. Cheng *et al.* proposed an actuator using the hybrid excitation. Compared with saw-tooth signal excitation, the step efficiency of the prototype was increased from 36.9% to 91.2% under the resonant/off-resonant hybrid excitation [25]. But the optimized waveform is often synthesized from a variety of simple signals, which is more complicated. Complex signals increase the cost and operation difficulty of the drive. In addition to the above two methods, in recent years, researchers have also used smart materials to reduce drawback [33], [34]. Wang *et al.* proposed an inertial piezoelectric actuator that used magnetorheological fluid to adjust friction, achieving the goal of no drawback, the prototype resolution reached 0.0204 μm [33]. This type of actuator also requires complex control signals, and the performance of the smart material itself needs to be studied. The sedimentation of the magnetorheological fluid also has an impact on the output performance of this type of actuator.

The above methods eliminate drawback only under certain working conditions. Aiming for a universal way of drawback control, this paper present a piezoelectric linear actuator controlled by the reversed-phase connection of two bimorphs. Two bimorphs of the actuator are asymmetrically clamped and connected in reversed-phase, so that the actuator always receives net force in the same direction. This method eliminates the backward phenomenon in principle, so there will be no backward under any frequency and voltage.

II. WORKING PRINCIPLE

A. STRUCTURE DESIGN

The structure of the piezoelectric actuator recommended in this paper is shown in Fig. 1. The actuator is mainly composed of a guide, a base plate, a load plate, two support frames, four short-clamping, two piezoelectric bimorphs and some bolts and nuts. The two piezoelectric bimorphs are fixed to the support frames with four short clamping plates by bolts and nuts.

B. MOVEMENT PROCESS

Piezoelectric actuators usually use one piezoelectric bimorph or two piezoelectric bimorphs that provide torque in the same direction. The actuator recommended in this article was connected by reversed-phase circuit. The positive pole of PZT1 and the negative pole of PZT2 are connected to the same end of the power supply, while the negative pole of PZT1 and the positive pole of PZT2 are connected to the other end of the power supply, as shown in Fig. 2(a). In this way, the two piezoelectric bimorphs will always bend in opposite directions. The excitation signal input is shown in Fig. 2(b). In Fig. 2(c), the two bimorphs are marked PZT1 (left) and PZT2 (right), respectively. A symmetric square wave is shared by the two reversed-phase connected bimorphs, which provides the reversed-phase exciting signal, as shown in Fig. 2(a). The vibration state of the two piezoelectric bimorphs is shown in Fig. 2(c). There are four stages in a cycle:

Holding stage I: The signal goes from "a" to "b" and the bimorphs hold the initial state.

Bending stage I: The signal goes from "b" to "c". Both bimorphs bend to the opposite position. According to previous studies [27], [29], the force pointing to the long-clamping direction is greater than that to the short-clamping direction.

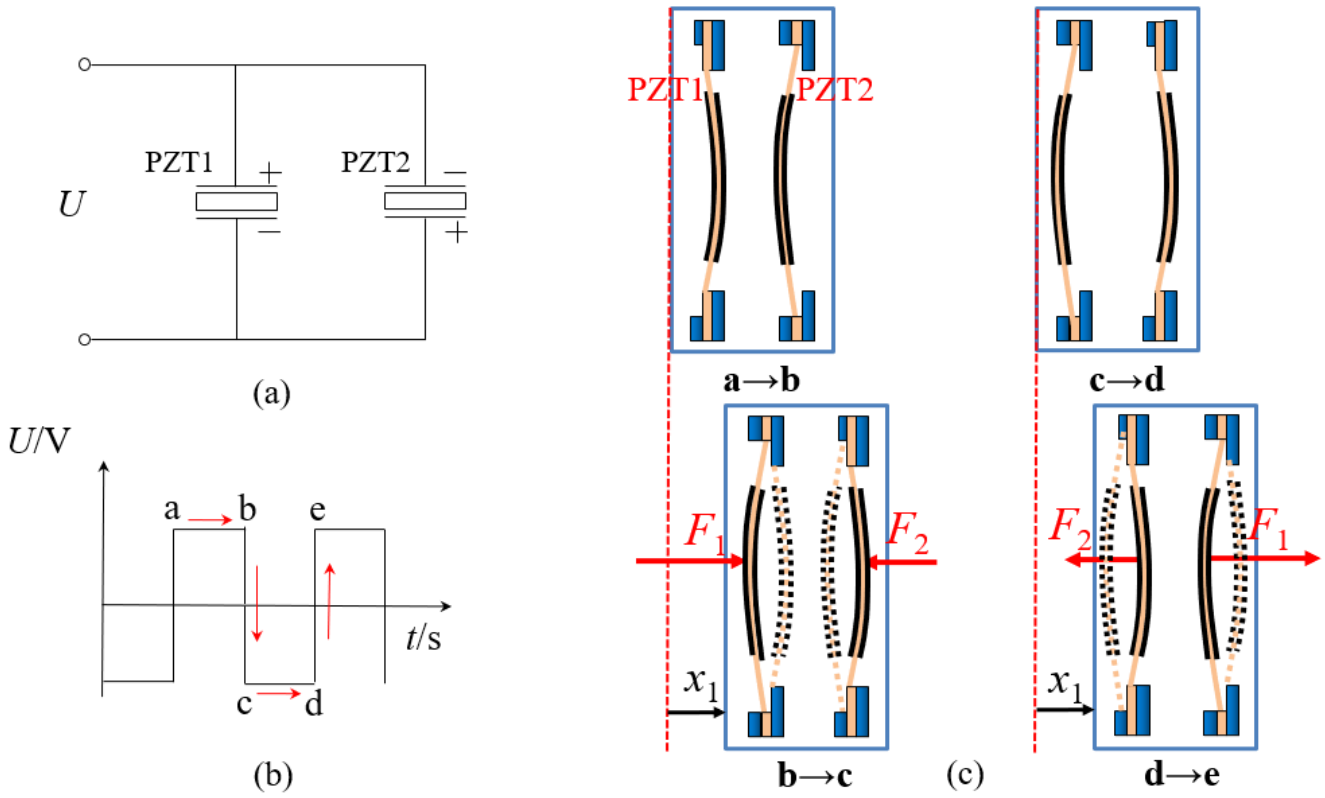

FIGURE 2. (a) Circuit diagram (b) Drive signal (c) Vibration state of piezoelectric bimorphs.

Then F_1 is greater than F_2. The net force $F_1 - F_2$ moves the actuator a displacement x_1 to the right, as shown in Fig. 2(c).

Holding stage II: The signal goes from "c" to "d" and the bimorphs hold the previous state.

Bending stage II: The signal goes from "d" to "e". Similar to bending stage I, the net force F_1- F_2 moves the actuator a displacement x_1 to the right, as shown in Fig. 2(c).

The actuator moves two steps in a cycle consisting of the above four stages. Drawback is theoretically eliminated as F_1 is greater than F_2. In case of bidirectional motion, another pair of piezoelectric bimorphs with short clampings on the right could be fixed on the same slider in parallel. This new pair of piezoelectric bimorphs will move the actuator to the opposite direction. Since the motion of the new pair works the same way to its counterpart, bidirectional motion is not further discussed in this study.

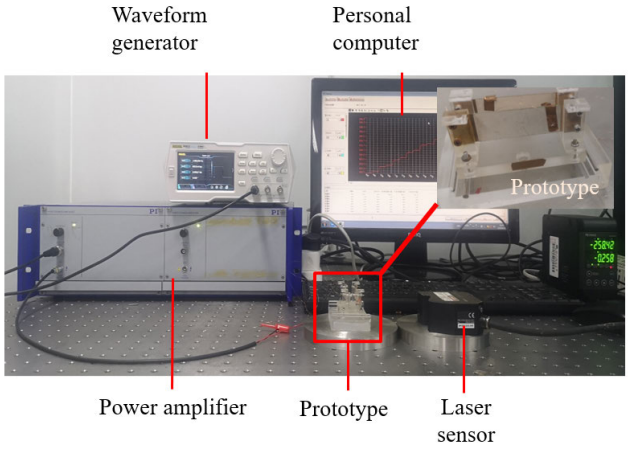

FIGURE 3. Components of the experimental system.

III. EXPERIMENT

A. EXPERIMENTAL SYSTEM

Fig. 3 illustrates the experimental system which consists of a waveform generator (RIGOL, DG812), a power amplifier (Physik Instrumente, E-472.20), a laser sensor (KEYENCE, LK-HD500), a personal computer and a prototype. The experimental system is placed on a vibration-isolated table. The waveform generator generates a square wave signal which is amplified by the power amplifier to drive the prototype. The displacement of the prototype is measured by the laser sensor and further processed with LK-Navigator software.

A zoomed picture of the prototype is shown in Fig. 3. The dimensional parameters and materials of the components are listed in Table 1. The load plate, the support frame, the base plate and the four short-clampings are all made of acrylic. The clamping difference between the long-clamping and short-clamping is 5 mm. The bolts and nuts are made of steel, and piezoelectric bimorphs are composed of PZT-5H and copper substrate. PZT 5H coupling factor: $K_p = 0.66$,

TABLE 1. Parts parameters are shown in table 1.

	L(mm)	H (mm)	W (mm)	Material
Prototype	80	44	50	N/A
Base	80	16	50	Acrylic
Slider	62	5	30	Acrylic
Load plate	62	2.5	32	Acrylic
Support frames	10	25	30	Acrylic
Short-clamping plate	5	15	2.5	Acrylic
Guide		Φ3×50		Carbon steel

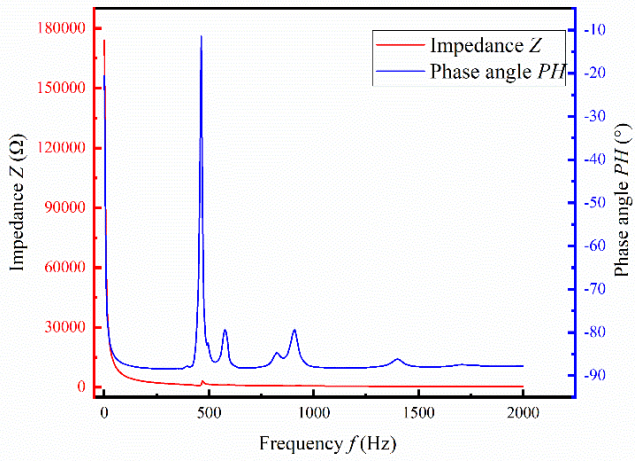

FIGURE 4. Impedance and response phase difference under different frequencies.

$K_{33} = 0.76$, $K_{31} = 0.38$, $K_t = 0.52$; The permittivity of PZT 5H is 3200; Piezoelectric coefficient: $d_{31} = 275 \times 10^{-12}$ C/N, $d_{33} = 620 \times 10^{-12}$ C/N, $g_{31} = 8.4 \times 10^{-3}$ Vm/N, $g_{33} = 20 \times 10^{-3}$ Vm/N; The poisson's ratio is 0.36. The track consists of 4 metal optical axes and acrylic, and 2 optical axes on both sides are used to guide the actuator to walk in a straight line.

B. FREQUENCY CHARACTERISTIC

Resonance frequency is an essential parameter to piezoelectric actuators. Resonant actuators work at resonance frequency for high transmission efficiency and output performance. Stepping actuators, usually non-resonant ones, try to keep away from the resonance frequency for sake of positioning precision. In order to find the resonance frequency of the prototype before frequency characteristic tests, an impedance analyzer was used to measure the impedance (Z) and the phase angle (PH) of the prototype at each frequency.

Fig. 4 shows the impedance and phase angle of the prototype at each frequency. Due to the lagging characteristic of the capacitance response, the steady response phase angle of the prototype is around $-87°$. When the frequency is 462 Hz, the response phase angle suddenly changes to about $-10°$, and the transmission efficiency reaches the maximum. It can be seen that the first order resonance frequency of the prototype is 462 Hz. Frequency characteristic of the actuator displacement peaks to 5.72 μm at 12 Hz. And the

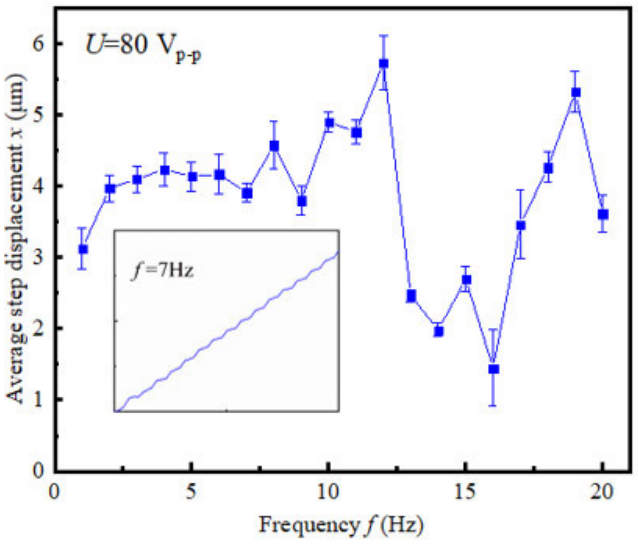

FIGURE 5. Average step displacement under different frequencies.

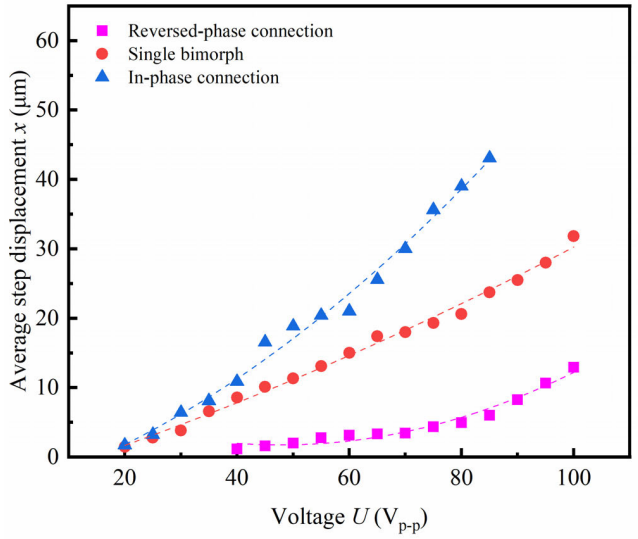

FIGURE 6. Average step displacement under different voltages with driving frequency of 2Hz.

average step at 80 Vp-p is illustrated in Fig. 5. It can be seen that the average step displacement reaches the minimum of 1.44 μm at 16 Hz. As frequency increases, there is no obvious law between the average step displacement and frequency. The stable range of frequency is from 2 to 7 Hz where the step displacements are all around 4 μm. Working frequency of the proposed actuator is recommended to select from this range.

C. VOLTAGE CHARACTERISTIC

Fig. 6 shows the voltage characteristic of piezoelectric actuators with in-phase connection, reversed-phase connection and single bimorph under the frequency of 2 Hz. The average step displacement increases as voltage goes up in all the three tests. At all voltages available for comparison, the average

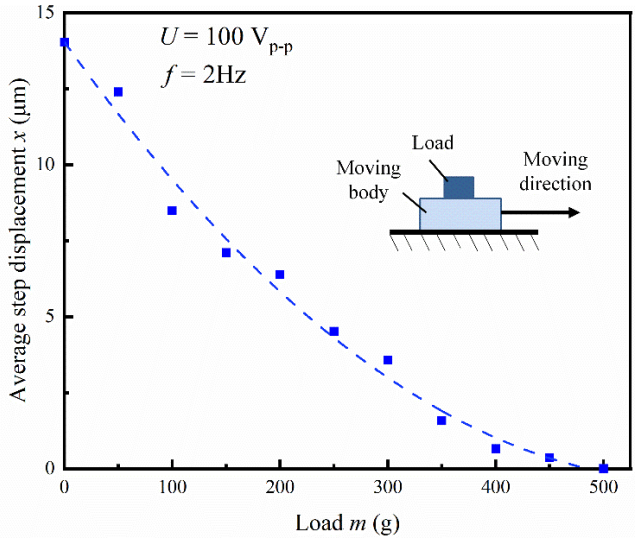

FIGURE 7. Average step displacement under different loads.

step displacement of in-phase connection is larger than that of single bimorph, and reversed-phase connection shows the smallest average step displacement. In addition, when the voltage is more than 80 V_{p-p}, the moment of inertia produced with in-phase connection far exceeds the moment of gravity, which causes the prototype to vibrate violently on the track, basically no forward displacement. The starting voltage of reversed-phase connection of reversed phase connection is 40 V_{p-p}, which is higher than the staring voltage of in-phase connection and single bimorph. The minimum average step displacement is 1.16 μm without load.

D. LOAD PERFORMANCE

In order to measure the output performance of the actuator, an investigation on the bearing capacity of the piezoelectric actuators was conducted. Fig. 7 shows the load characteristic of the piezoelectric actuator under the frequency of 2 Hz and the driving voltage of 100 V_{p-p}. Obviously, the average step displacement decreases as load is increased and the actuator cannot work with the load above 450 g. The minimum average step displacement of the actuator controlled by reversed-phase connection is 0.725 μm by 450-g load.

E. OUTPUT STEPPING CHARACTERISTIC

Stepping characteristic test aims to verify the basic features of reversed-phase connection excitation: two steps each cycle and zero drawback. This experiment is conducted at a frequency of 2 Hz, a voltage range of 40-80 V_{p-p} and no load. Fig. 8 shows the output stepping characteristic of the actuator. This figure illustrates that the actuator moves two steps forward regularly without drawback, and the output movement is relatively stable.

F. LINEARITY CHARACTERISTIC

Fig. 9 shows the stepping characteristic curve of the actuator at the frequency of 1 Hz, 2 Hz and 3 Hz under 80 V_{p-p}.

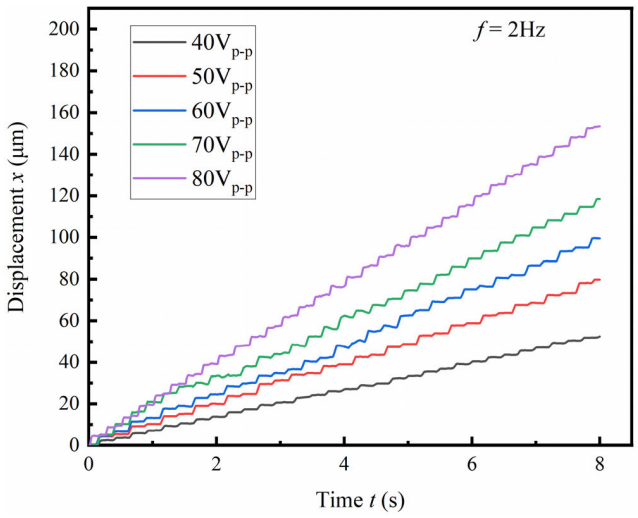

FIGURE 8. Displacement history at different voltages.

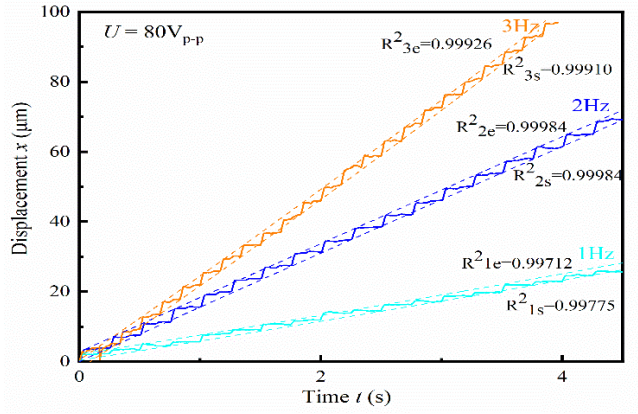

FIGURE 9. Displacement history at 1 Hz, 2 Hz, 3 Hz.

In order to compare the linearity of the stepping curves, linear fitting was conducted for both the start and end point of each step. The dotted line below the stepping curve represents the fitting line of start points, marked R^2s, and the dotted line above the stepping curve represents the fitting line of end points, marked R^2e. R-squares of linear fittings of all three frequencies are above 0.99, demonstrating a good linearity. This indicates that the actuator works quite stable at the selected test conditions. The maximum R-square is 0.99984 happening at 2 Hz.

G. REPEATABILITY

Repeatability is an important indicator to evaluate the stability of piezoelectric. Two indexes, fluctuation range and standard deviation, are selected to verify the repeatability of the proposed actuator. Fluctuation range is calculate d with equation 1:

$$R = x_{max} - x_{min} \tag{1}$$

where x_{max} and x_{min} are the maximum and minimum value of the 10 repeat tests.

TABLE 2. Performance comparison of actuators with different mechanisms.

Author	Minimum average step displacement	Drawback rate	Number of signals	Number of steps in each cycle	The method of Controlling drawback
He *et al.* [18]	1.14 μm	N/A	2	1	N/A
Zhang *et al.* [28]	0.6 μm	Sometimes 0%	1	1	Adjusting structural parameters and voltage
Cheng *et al.* [29]	0.85 μrad	24%	1	1	N/A
Wang *et al.* [32]	N/A	Decreased by 83% and 85%	A composite waveform	1	Optimizing the waveform
Wang *et al.* [33]	0.0204 μm	Sometimes 0%	1	1	MRF control friction
Wen *et al.* [34]	0.1 μm	Sometimes 0%	2	1	MRF control friction
Lu *et al.* [35]	0.453 μrad	90.6%	1	1	N/A
This paper	0.725 μm	0%	1	2	Reversed-phase connection

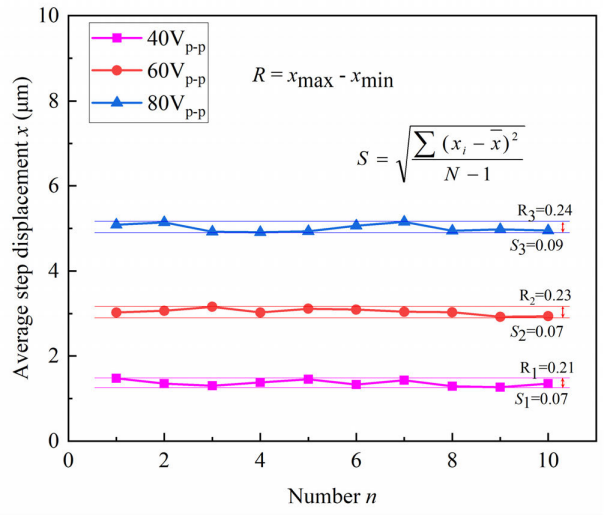

FIGURE 10. Repetitive experiment with driving frequency of 2 Hz.

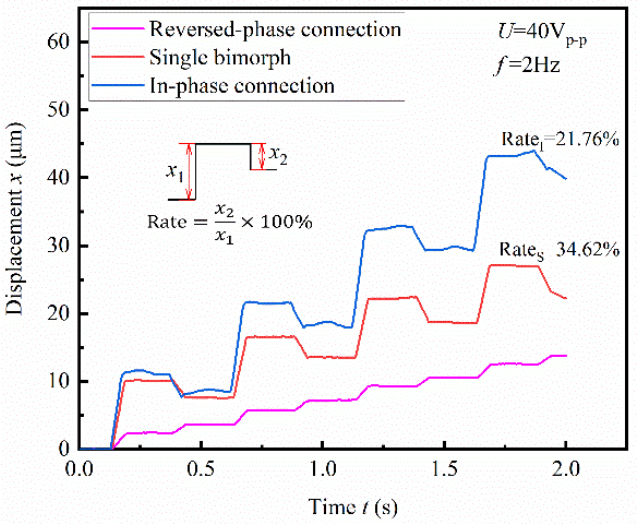

FIGURE 11. Displacement history of different connections.

Standard deviation S is defined by equation 2:

$$S = \sqrt{\frac{\sum (x_i - \overline{x})^2}{N - 1}} \tag{2}$$

where N denotes the number of repetitions, x_i is the average step displacement of the i_{th} experiment, and $\overline{x}$ is the average step displacement of N experiment times. The experiment repeated 10 times with voltages of 40, 60, 80 V_{p-p} and the frequency of 2 Hz. Each test recorded 20 steps started from the same position. As shown in Fig. 10, both fluctuation range and standard deviation decrease as the voltage goes lower. The standard deviation is reduced from 0.09 to 0.07 μm and the fluctuation range is reduced from 0.24 to 0.21 μm.

IV. DISCUSSION

A. COMPARISION OF IN-PHASE CONNECTION AND REVERSED-PHASE CONNECTION

In order to better understand the influence of bimorph connections, the output stepping characteristics of in-phase connection, reversed-phase connection and single bimorph were tested under the frequency of 2 Hz and the voltage of 40 V_{p-p}. As shown in Fig. 11, both in-phase connection and single bimorph move a big step forward and a small step backward, whereas reversed-phase connection moves two steps forward. Reversed-phase connection eliminates drawback.

The drawback rate, formula is as follows:

$$Rate = \frac{x_2}{x_1} \times 100\% \tag{3}$$

where x_1 represents the forward average step displacement, x_2 is the average step displacement of drawback. The drawback rate of actuator by one single bimorph is 34.62%, and the drawback rate of actuator by in-phase connection is 21.76%. In addition, the resolution of actuator by reversed-phase connection is higher than that of in-phase connection and single bimorph, which makes reversed-phase connected actuators suitable for precise positioning.

B. COMPARISION WITH OTHER ACTUATORS

Table 2 shows the performance comparison of the proposed and other actuators. The actuator proposed in this paper can motion without drawback in any state by a simple control signal, and it moves forward two steps in a cycle. In addition, the actuator proposed in this article is also competitive in minimum average step displacement.

Although reversed-phase connection demonstrates good performance for asymmetric clamping piezoelectric actuators, it is not a universal way of eliminating drawback for inertial piezoelectric actuators. The key factor of reversed-phase connection is to neutralize the backward force by the forward force, which demands simultaneous actions of the two piezoelectric elements. For stick-slip actuators, e.g. sawtooth ones, the forward impact force happens instantly, but the backward impact force lasts for a short period. Neutralization in this case can hardly be fully reached. Thus it is not applicable to every piezoelectric actuator.

V. CONCLUSION

A piezoelectric linear actuator with two asymmetrically clamped bimorphs in reversed-phase connection is presented in this paper. Characteristic tests were conducted on a prototype with the proposed connection. Comparison tests of in-phase connection, reversed-phase connection and single bimorph were also provided. The following conclusions are verified by experiments:

1) The piezoelectric actuator driven by reversed-phase connection can move forward two steps in a straight line each cycle without drawback.

2) The maximum load of the actuator is 450 g with a 100-V_{p-p} voltage, a 2-Hz frequency, and the average step displacement in this case is 0.725 μm.

3) The proposed actuator shows preferable repetition in terms of fluctuation range and standard deviation.

REFERENCES

[1] L. Wang, Y. Hou, K. Zhao, H. Shen, Z. Wang, C. Zhao, and X. Lu, "A novel piezoelectric inertial rotary motor for actuating micro underwater vehicles," *Sens. Actuators A, Phys.*, vol. 295, pp. 428–438, Aug. 2019.

[2] H. Jalili, G. Vossoughi, and H. Salarieh, "Motion analysis of a vibrational micro-robot with two perpendicular harmonic actuators and deriving the design parameters in stick-slip-jump mode," *J. Sound Vibrat.*, vol. 372, pp. 266–282, Jun. 2016.

[3] S. Chopra and N. Gravish, "Piezoelectric actuators with on-board sensing for micro-robotic applications," *Smart Mater. Struct.*, vol. 28, no. 11, Nov. 2019, Art. no. 115036.

[4] C. Belly and W. Charon, "Benefits of amplification in an inertial stepping motor," *Mechatronics*, vol. 22, no. 2, pp. 177–183, Mar. 2012.

[5] Y. Yoda, K. Okada, H. Wang, S. P. Cramer, and M. Seto, "High-resolution monochromator for iron nuclear resonance vibrational spectroscopy of biological samples," *Jpn. J. Appl. Phys.*, vol. 55, no. 12, Dec. 2016, Art. no. 122401.

[6] I. Mannhardt, C. Warncke, H. K. Trieu, J. Müller, and T. Eschenhagen, "Piezo-bending actuators for isometric or auxotonic contraction analysis of engineered heart tissue," *J. Tissue Eng. Regenerative Med.*, vol. 13, no. 1, pp. 3–11, Jan. 2019.

[7] K. H. Koh, T. Kobayashi, J. Xie, A. Yu, and C. Lee, "Novel piezoelectric actuation mechanism for a gimbal-less mirror in 2D raster scanning applications," *J. Micromech. Microeng.*, vol. 21, no. 7, Jul. 2011, Art. no. 075001.

[8] S.-H. Chen, A. Michael, and C. Y. Kwok, "Design and modeling of piezoelectrically driven micro-actuator with large out-of-plane and low driving voltage for micro-optics," *J. Microelectromech. Syst.*, vol. 28, no. 5, pp. 919–932, Oct. 2019.

[9] H. Wang and L. Hu, "Linear and nonlinear analysis of the thermal effects of beam piezoelectric bending actuator on adaptive optics," *J. Intell. Mater. Syst. Struct.*, vol. 28, no. 20, pp. 3016–3024, Dec. 2017.

[10] A. Xu, Q. Gu, and H. Yu, "Mechanism of controllable force generated by coupling inverse effect of piezoelectricity and magnetostriction," *Int. J. Precis. Eng. Manuf.-Green Technol.*, to be published, doi: 10.1007/s40684-020-00223-5.

[11] Z. Zhu, H. Du, R. Zhou, P. Huang, W.-L. Zhu, and P. Guo, "Design and trajectory tracking of a nanometric ultra-fast tool servo," *IEEE Trans. Ind. Electron.*, vol. 67, no. 1, pp. 432–441, Jan. 2020.

[12] Y. Tian, B. Shirinzadeh, and D. Zhang, "A flexure-based mechanism and control methodology for ultra-precision turning operation," *Precis. Eng.*, vol. 33, no. 2, pp. 160–166, Apr. 2009.

[13] J. Li, X. Zhou, H. Zhao, M. Shao, P. Hou, and X. Xu, "Design and experimental performances of a piezoelectric linear actuator by means of lateral motion," *Smart Mater. Struct.*, vol. 24, no. 6, Jun. 2015, Art. no. 065007.

[14] F. Qin, G. Dai, X. Sun, Q. Xu, Y. Du, and J. Bao, "A novel PZT-based traveling-wave micromotor with high performance and unconstrained coaxial rotation," *J. Microelectromech. Syst.*, vol. 27, no. 4, pp. 635–642, Aug. 2018.

[15] Y. Liu, J. Deng, and Q. Su, "Review on multi-degree-of-freedom piezoelectric motion stage," *IEEE Access*, vol. 6, pp. 59986–60004, 2018.

[16] A. Čeponis and D. Mažeika, "An inertial piezoelectric plate type rotary motor," *Sens. Actuators A, Phys.*, vol. 263, pp. 131–139, Aug. 2017.

[17] K. Chen, J. Wen, G. Cheng, J. Ma, and P. Zeng, "An asymmetrical inertial piezoelectric rotary actuator with the bias unit," *Sens. Actuators A, Phys.*, vol. 251, pp. 179–187, Nov. 2016.

[18] D. Shen, J. Wen, J. Ma, Y. Hu, R. Wang, and J. Li, "A novel linear inertial piezoelectric actuator based on asymmetric clamping materials," *Sens. Actuators A, Phys.*, vol. 303, Mar. 2020, Art. no. 111746.

[19] J. Wen, K. Chen, J. Ma, J. Zheng, and G. Cheng, "Theoretical modeling and experimental validation of inertial piezoelectric actuators," *IEEE Access*, vol. 7, pp. 19881–19889, 2019.

[20] H. Bao, J. Wen, K. Chen, J. Ma, D. Lei, and J. Zheng, "An inertial piezoelectric hybrid actuator with large angular velocity and high resolution," *J. Intell. Mater. Syst. Struct.*, vol. 30, no. 14, pp. 2099–2111, Aug. 2019.

[21] Y. Hu, R. Wang, J. Wen, and J.-Q. Liu, "A low-frequency structure-control-type inertial actuator using miniaturized bimorph piezoelectric vibrators," *IEEE Trans. Ind. Electron.*, vol. 66, no. 8, pp. 6179–6188, Aug. 2019.

[22] L. Xiaotao, Y. Zhigang, and L. Jianfang, "Research on a piezoelectric actuator based on the match of impact and friction," in *Proc. Int. Colloq. Comput., Commun., Control, Manage. (ISECS)*, Aug. 2009, pp. 8–9.

[23] L. He, Y. Chu, S. Hao, X. Zhao, Y. Dong, and Y. Wang, "Inertial piezoelectric linear motor driven by a single-phase harmonic wave with automatic clamping mechanism," *Rev. Sci. Instrum.*, vol. 89, no. 5, May 2018, Art. no. 055008.

[24] J. Wen, J. Ma, P. Zeng, G. Cheng, and Z. Zhang, "A new inertial piezoelectric rotary actuator based on changing the normal pressure," *Microsyst. Technol.*, vol. 19, no. 2, pp. 277–283, Feb. 2013.

[25] T. Cheng, H. Li, M. He, H. Zhao, X. Lu, and H. Gao, "Investigation on driving characteristics of a piezoelectric stick–slip actuator based on resonant/off-resonant hybrid excitation," *Smart Mater. Struct.*, vol. 26, no. 3, Mar. 2017, Art. no. 035042.

[26] H. Huang, H. Zhao, Z. Yang, J. Mi, Z. Fan, S. Wan, C. Shi, and Z. Ma, "A novel driving principle by means of the parasitic motion of the micro-gripper and its preliminary application in the design of the linear actuator," *Rev. Sci. Instrum.*, vol. 83, no. 5, May 2012, Art. no. 055002.

[27] Y. Zhang, M. Wang, Y. Cheng, D. Zheng, and Y. Peng, "A stick-slip/inchworm hybrid rotary piezo motor based on a symmetric triangular driving mechanism," *Appl. Phys. Lett.*, vol. 115, no. 13, Sep. 2019, Art. no. 131904.

[28] S. Wang, W. Rong, L. Wang, Z. Pei, and L. Sun, "Design, analysis and experimental performance of a novel stick-slip type piezoelectric rotary actuator based on variable force couple driving," *Smart Mater. Struct.*, vol. 26, no. 5, May 2017, Art. no. 055005.

[29] E. Zhang, Y. Hu, H. Bao, J. Li, J. Ma, and J. Wen, "A linear inertial piezoelectric actuator using a single bimorph vibrator," *Smart Mater. Struct.*, vol. 28, no. 11, Nov. 2019, Art. no. 115020.

[30] G. Cheng, Y. Hu, J. Wen, P. Zeng, and C. Xing, "Piezoelectric inertial rotary actuators based on asymmetrically clamping structures," *Sens. Actuators A, Phys.*, vol. 223, pp. 125–133, Mar. 2015.
[31] L. Wang, D. Chen, T. Cheng, P. He, X. Lu, and H. Zhao, "A friction regulation hybrid driving method for backward motion restraint of the smooth impact drive mechanism," *Smart Mater. Struct.*, vol. 25, no. 8, Aug. 2016, Art. no. 085033.
[32] L. Wang, W. Chen, J. Liu, J. Deng, and Y. Liu, "A review of recent studies on non-resonant piezoelectric actuators," *Mech. Syst. Signal Process.*, vol. 133, Nov. 2019, Art. no. 106254.
[33] R. Wang, Y. Hu, D. Shen, J. Ma, J. Wen, and J. Li, "Design and experimental performance of a novel piezoelectric inertial actuator for magnetorheological fluid control using permanent magnet," *IEEE Access*, vol. 7, pp. 43573–43580, 2019.
[34] J. Wen, D. Shen, R. Wang, J. Li, and J. Ma, "A two-fixed-end beam piezoelectric inertial actuator using electromagnet controlled magnetorheological fluid (MRF) for friction regulation," *Smart Mater. Struct.*, vol. 29, no. 6, Jun. 2020, Art. no. 065011.
[35] Q. Lu, J. Wen, Y. Hu, K. Chen, H. Bao, and J. Ma, "Novel inertial piezoelectric actuator with high precision and stability based on a two fixed-end beam structure," *Smart Mater. Struct.*, vol. 28, no. 1, Jan. 2019, Art. no. 015030.
[36] R. Wang, Y. Hu, D. Shen, J. Ma, J. Li, and J. Wen, "A novel piezoelectric inchworm actuator driven by one channel direct current signal," *IEEE Trans. Ind. Electron.*, vol. 68, no. 3, pp. 2015–2023, Mar. 2021.

TIANYU JIANG was born in Chuzhou, China, in 1999. He is currently pursuing the bachelor's degree with Zhejiang Normal University, Jinhua, China. His main research interest includes piezoelectric drive.

JIJIE MA received the B.Sc. degree in automation from Dalian Maritime University, China, in 2003, and the M.S. and Ph.D. degrees in mechanical engineering from Jilin University, China, in 2006 and 2010, respectively. He is currently an Associate Professor with Zhejiang Normal University. He has published more than ten scientific papers. His main research interest includes precision machinery.

YILI HU was born in Hangzhou, China, in 1989. He received the B.S. degree in mechanical design, manufacturing and automation and the M.S. degree in physical electronics from Zhejiang Normal University, Jinhua, China, in 2008 and 2012, respectively, and the Ph.D. degree from Shanghai Jiao Tong University, Shanghai, China, in 2020.

He is currently working as a Lecturer with Zhejiang Normal University. His current research interests include piezoelectric actuators, sensors, and energy harvesters.

QITAO LU was born in Jiaxing, China, in 1996. He received the B.S. degree in mechanical design, manufacturing and automation from Zhejiang Normal University, Jinhua, China, in 2019, where he is currently pursuing the M.S. degree in mechanical and electrical engineering. His research interests include piezoelectric drive and control technology.

JIANPING LI was born in Jiangsu, China, in 1987. He received the B.S. and Ph.D. degrees from the School of Mechanical Science and Engineering, Jilin University, Changchun, China, in 2011 and 2016, respectively.

He worked with Chiba University, Japan, as a JSPS Researcher, supported by the Japan Society for the Promotion of Science (JSPS). Since 2018, he has been working with the Institute of Precision Machinery and Smart Structure, College of Engineering, Zhejiang Normal University. His current research interests include piezoelectric actuator-based nano-positioning systems and the application of electrical impedance spectroscopy in biomedical science.

JIANMING WEN was born in 1980. He received the B.Sc., M.Sc., and Ph.D. degrees from Jilin University, in 2003, 2006, and 2009, respectively. He is currently a Professor with Zhejiang Normal University, China. He has published more than 40 scientific articles. His main research interests include piezoelectric drive and control technology.